IMAACA'2004

Model Predictive Control of Solid Substrate Cultivation Bioreactors

Mario Fernández
Departamento de Ciencias de la Ingeniería
Universidad de Talca
Camino a Los Niches Km.1, Curicó, CHILE
Phone: +56-75-325955, Fax: +56-75-325958, E-mail: mafernandez@utalca.cl

Ricardo Pérez-Correa
Departamento de Ingeniería Química y Bioprocesos
Pontificia Universidad Católica de Chile
Vicuña Mackenna 4860, Santiago, CHILE
Phone: +56-2-3544258, Fax: +56-2-3545803, E-mail: perez@ing.puc.cl

Keywords: SSC; SSF; Evaporative cooling, Fermentation; Modeling; Multivariable control.

Abstract - The design and operation of large scale Solid Substrate Cultivation (SSC) bioreactors is difficult, therefore, it is not possible to operate well this kind of bioreactors without automatic control. In addition, conventional control systems (decoupling PID, split range, etc.) do not perform properly, since the controllers must be retuned during the cultivation process, the control strategy must be adapted according to the process response, and is not always possible to deal well with input constraints. Here we present simulation results regarding the application of Linear Model Predictive Control (LMPC) for the operation of large scale SSC bioreactors. A phenomenological nonlinear dynamic model was calibrated using real time data coming from pilot scale SSC bioreactor cultivations. The bioreactor model was coded in Simulink and the MPC Graphical User Interface for the MPC toolbox of Matlab was used to run the control simulations.

I. PROCESS MODEL

Process Description

Simulations in this paper were performed with a model of a 200 kg capacity aseptic pilot SSC bioreactor (Fig. 1). The bioreactor was used for cultivations of the fungus *Gibberella fujikuroi* on wheat bran to produce Gibberellic acid. For optimum growth and production, bed water content should be raised from 50% and stabilized at 70% after the growth phase. In addition, bed temperature should be held constant at 28°C. As is common practice in large scale SSC bioreactors, evaporative cooling is applied for temperature control; here, inlet air flowrate, temperature, and relative humidity are manipulated simultaneously. This control technique implies large moisture losses and should therefore be combined with periodic addition of fresh water in combination with agitation as described in detail in [Fernández et al., 1997] and [Peña y Lillo et al., 2001]. Agitation was turned on either when fresh water was added, or when the temperature gradient in the bed exceeded 10ºC. The main measured variables were: inlet air flow rate, G, inlet and outlet air temperatures, T_{gi} and T_{go}, inlet air relative humidity, H_{gi}, outlet air CO_2 and O_2 concentration, and the bed-temperature at six different

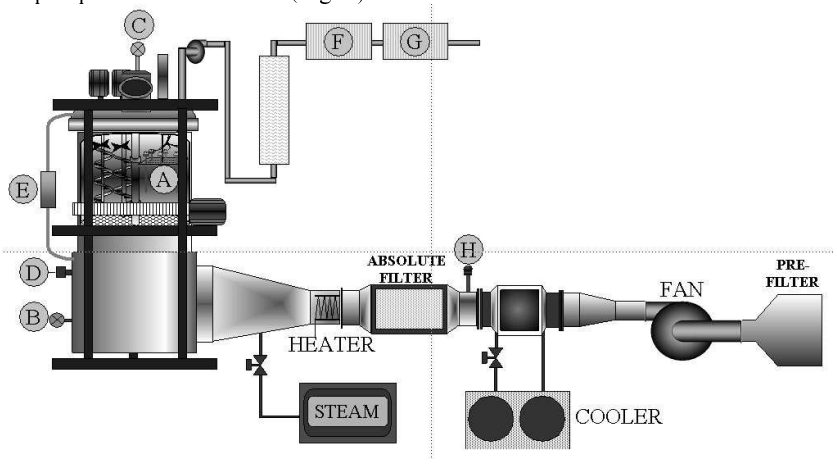

Fig. 1. Instrumentation of the SSC bioreactor. A: six thermocouples (bed temperature); B: thermocouple (inlet air temperature); C: thermocouple (outlet air temperature); D: Relative humidity transmitter (inlet air relative humidity); E: DP transmitter (drop pressure); F: CO_2 IR detector (CO_2 concentration); G: O_2 paramagnetic detector (O_2 concentration); H: anemometer.

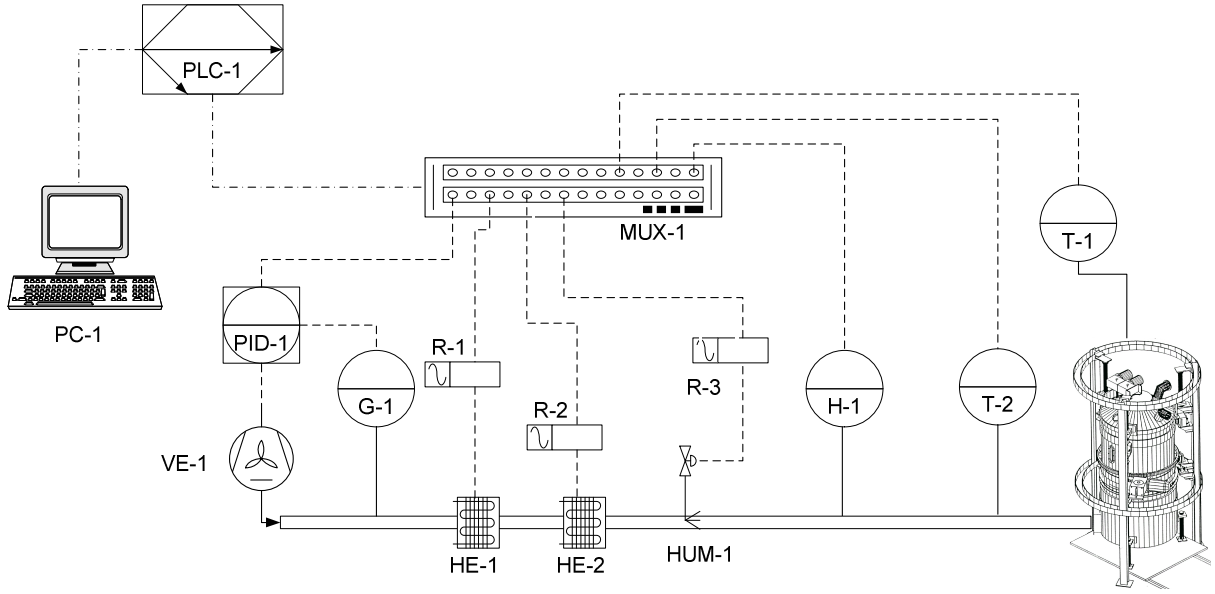

Fig. 2. Average bed temperature control system. The system comprises three inner loops: (1) Inlet air (G-1) is controlled by the fan speed (VE-1) with a PID; (2) Inlet air temperature (T-2) is controlled by a chiller (HE-1) and a heater (HE-2) using relays R-1 and R-2 respectively; (3) Inlet air relative humidity (H-1) is controlled by vapor addition (HUM-1) using relay R-3. The external loop controls the average bed temperature (T-1) by simultaneous manipulation of the inlet air flowrate, relative humidity and temperature. A programmable logic controller (PLC-1) supervises the basic control actions (PID and On/Off) and a personal computer (PC-1) is used by the operator and process engineer for manual control, process supervision, data storage and management, set point changes, plant start up and shut down, definition of control loops and coding of advanced controllers. Refer to [Fernández, 2001] for further details.

locations. These variables were measured on-line at a sampling rate of 20 s. The bed-water content, X_W, was measured from samples taken manually approximately every 4 h. Water seepage from the bottom of the reactor, W_P, was estimated from infrequent manual measurements. Dry mass was also measured manually at the beginning and at the end of the fermentation. Fig. 2 shows the control structure used to regulate the average bed temperature.

A simple lumped parameter model that reproduces the main features of the dynamic response of this reactor is presented next. Due to space limitations, only the main equations of the model are given here. The interested reader can find the complete model in [Peña y Lillo et al., 2001], [Lekanda and Pérez-Correa, 2004] and [Fainé, 2004].

Kinetics

The experimentally measured biomass corresponds to the total amount of biomass, X_{tot}, considering active and inactive fungi and is expressed on dry mass basis (kg $_{d.b.}$) by:

$$\frac{dX_{tot}}{dt} = \mu X \qquad [kg_X/h \cdot kg_{d.b.}] \qquad (1)$$

where μ represents the specific growth rate. Assuming a first order death rate, the active biomass, X, (which is the total biomass minus the inactive biomass) is described by:

$$\frac{dX}{dt} = \mu X - \delta X \qquad [kg_X/h \cdot kg_{d.b.}] \qquad (2)$$

where δ represents the specific death rate.

Gibberella fujikuroi accumulates part of the primary nitrogen source and uses this nutrient for biomass growth when the external source has been depleted. Considering that wheat bran degradation follows zero order kinetics, the consumption rate of the primary nitrogen source is given by:

$$\frac{dN}{dt} = -k \qquad [kg_N/h \cdot kg_{d.b.}] \qquad (3)$$

where k is the conversion factor between wheat bran nitrogen and available nitrogen for the microorganism (N_I).

The change in available nitrogen is expressed by:

$$\frac{dN_I}{dt} = \phi \cdot k - \mu \cdot \left(\frac{X}{Y_{X/N_I}} \right) \qquad [kg_N/h \cdot kg_{d.b.}] \qquad (4)$$

where ϕ is the nitrogen percentage in wheat bran that is assimilated by the microorganism and $Y_{X/N}$ is the mass yield between biomass growth and available nitrogen.

The evolution of respiratory gases can be described by two terms. The first is associated with the growth of the microorganism and the second with its maintenance, as described in [Gelmi et al., 2002]. Then, the CO_2 production and O_2 consumption rates on a dry mass basis is given by:

$$\frac{dCO_2}{dt} = \mu \cdot \frac{X}{Y_{X/CO_2}} + m_{CO_2} \cdot X \qquad [kg_{CO_2}/h \cdot kg_{d.b.}] \tag{5}$$

$$\frac{dO_2}{dt} = \mu \cdot \frac{X}{Y_{X/O_2}} + m_{O_2} \cdot X \qquad [kg_{O_2}/h \cdot kg_{d.b.}] \tag{6}$$

Dry mass consumption is expressed by a linear relationship between a degradation coefficient obtained empirically, k_g, and the CO_2 production rate, CPR:

$$\frac{dMs}{dt} = -k_g \cdot CPR \cdot Ms \qquad [kg_{d.b.}/h] \tag{7}$$

The specific growth rate, μ, considers the effect of the limiting nutrient (intermediary nitrogen) on biomass growth, using a Monod's rate expression:

$$\mu = \frac{\mu_M N_I}{(N_I + k_N)} \qquad [1/h] \tag{8}$$

where μ_M is the maximum specific growth rate and k_N is the substrate inhibition constant.

Energy and water balances

The model assumes that the outlet gas is saturated, that there is no accumulation in the gas phase and that the atmospheric pressure, P_{atm}, remains constant and equal to 760 mmHg.

The evaporation rate, E, calculated on a dry mass basis, is given by:

$$E = \frac{G \cdot (Y_{go} - Y_{gi})}{Ms} \qquad [kg_w/h \cdot kg_{d.b.}] \tag{9}$$

where Y_{go} and Y_{gi} are the humidities of the outlet and inlet air respectively.

The average water content of the bed, X_W, is given by,

$$\frac{dX_W}{dt} = R_W - E + \frac{F_W - Wp}{Ms} - \frac{X_W}{Ms} \cdot \frac{dMs}{dt} \qquad [kg_w/h \cdot kg_{d.b.}] \tag{10}$$

This equation includes metabolic water production, R_W, addition of fresh water, F_W, evaporation losses, E, and seepage through the lower part of the reactor, Wp. The last term in the balance equation represents substrate degradation since X_W is expressed on a dry mass basis.

The metabolic water generation is expressed on a dry mass basis by a correlation between the CO_2 production rate and a conversion factor, k_W:

$$R_W = \frac{(k_W \cdot CPR)}{Ms} \qquad [kg_w/h \cdot kg_{d.b.}] \tag{11}$$

The change in the bed-temperature can be obtained from the balance equation and is given by:

$$\frac{dT_b}{dt} = \frac{1}{Cs \cdot k_{\exp}} \cdot (Q_{F_W} + \Delta Hr + Q_{O_2} - Q_{CO_2} - Q_g - Q_{wall}) [^\circ C/h] \tag{12}$$

The terms included here are metabolic heat generation, ΔHr, heat removed by the gas, Q_g, heat losses through the reactor wall, Q_{wall}, and the enthalpy contribution of added water, Q_{Fw}.

The metabolic heat production can be related to the evolution of respiratory gases by:

$$\Delta Hr = -Y_{q/CO_2} \cdot CPR \qquad [J/h] \tag{13}$$

The heat removed by the gas, Q_g, is calculated choosing 0ºC as the reference temperature. The transfer phenomena mechanisms considered are evaporation losses, Q_{evap}, forced convection between the bed and the airflow, Q_{conv}, and sensible heats associated with respiratory gases (Q_{O2} and Q_{CO2}).

Evaporation losses are given by:

$$Q_{evap} = G \cdot \lambda_w \cdot (Y_{go} - Y_{gi}) \qquad [J/h] \tag{14}$$

The forced air convection can be estimated from:

$$Q_{conv} = G \cdot \begin{bmatrix} C_{P,a} \cdot (T_{go} - T_{gi}) + C_{P,v} \cdot (Y_{go} \cdot T_{go} - Y_{gi} \cdot T_{gi}) \\ - C_{P,v} \cdot T_b \cdot (Y_{go} - Y_{gi}) \end{bmatrix} [J/h] \tag{15}$$

where the outlet gas temperature is defined by the heat transfer between the solid and the gas.

$$Q_g = A \cdot h_S \cdot (T_b - T_{go}) \tag{16}$$

Heat transfer through the reactor walls is by natural convection and radiation:

$$Q_{wall} = A \cdot \left[h \cdot (T_{wall} - T_{amb}) + \sigma \cdot \xi \cdot \begin{pmatrix} (T_{wall} + 273.15)^4 \\ -(T_{amb} + 273.15)^4 \end{pmatrix} \right] [J/h] \quad (17)$$

The values of the model parameters used in the simulations are giving in the appendix.

II. MODEL CALIBRATION

This model was coded in Simulink/Matlab™ and fitted with data coming from a fermentation run performed in the SSC pilot bioreactor described above. Kinetic parameters were taken from [Lekanda and Pérez-Correa, 2004] and the energy and water balance parameters were taken from [Peña y Lillo et al., 2001]. It was found by [Fainé, 2004] that the model is mostly sensitive to k_g, Y_{XCO2}, k_w and $Y_{X/Ni}$. Here, these parameters were heuristically fitted to the data. Calibration results are shown in figures 3 to 7 and model parameters are given in the appendix.

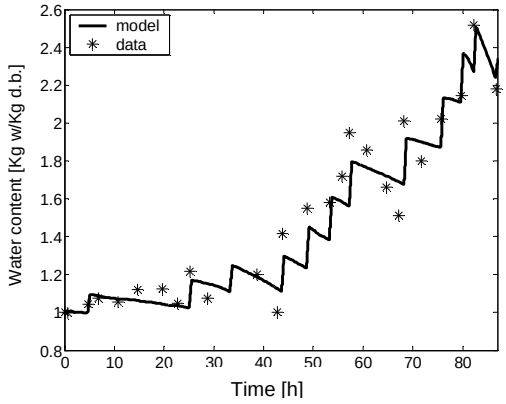

Fig. 3. Evolution of the bed water content.

The model fitting shown in Fig. 3 looks reasonable, considering that water content measurements were prone to large errors due to sampling a highly heterogeneous medium.

The temperature shown in Fig. 4 is the average of the six measurements inside the bed. Hence, the dynamics it shows is partly due to the heterogeneity of the bed, particularly during the first 30 hours, where the heat generation rate is high. The simplified lumped parameter model reproduces the trend of the observed bed temperature, but it can't reproduce the effect of bed heterogeneity.

The simulated outlet temperature (Fig. 5) also presents high oscillations during the first 20 hours, mainly due to channeling, hot and cold spots inside the bed. These effects are impossible to reproduce by lumped parameter models. Despite this, the model reproduces well the trend of the observed values.

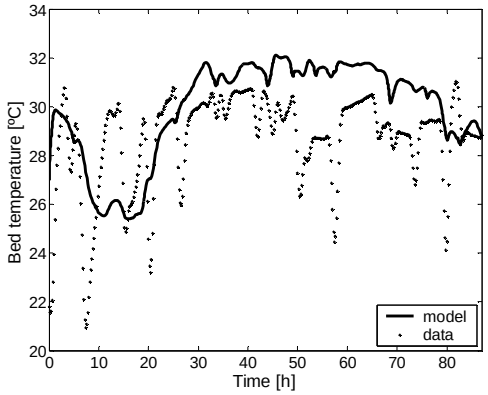

Fig. 4. Evolution of the average bed temperature.

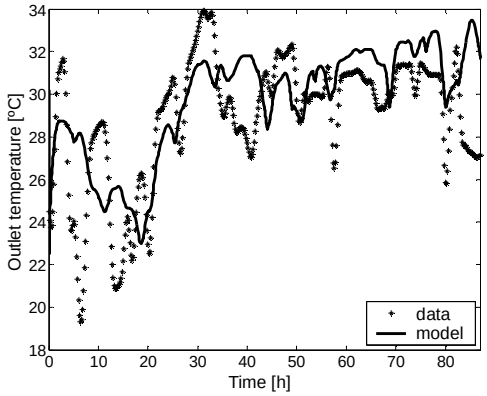

Fig. 5. Evolution of the outlet air temperature.

The CO_2 production rate shown in Fig. 6 is reproduced in average by the model. However, the model cannot reproduce the high peaks and oscillations caused by heterogeneity, agitation, gas occlusion and by the uneven colonization of the solid bed by the microorganism.

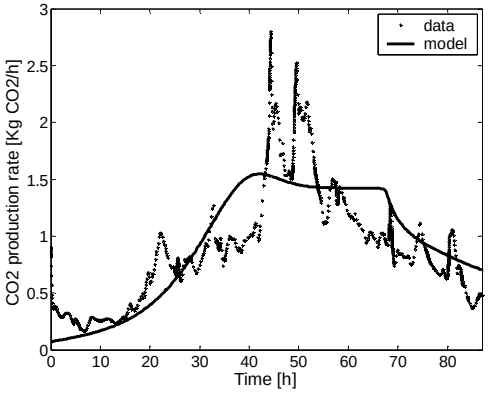

Fig. 6. Evolution of the CO_2 production rate.

The total CO_2 produced is not much sensitive to bed heterogeneity, therefore the model and data curves shown in Fig. 7 are closer than the curves shown in the previous figures.

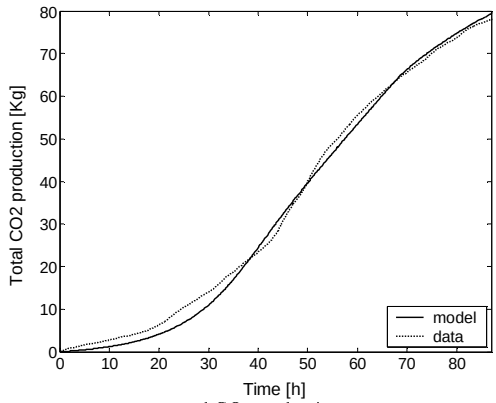

Fig. 7. Total CO_2 production.

Of course an improved overall fitting can be obtained with more tuning, or even better, with an optimization routine. However, for automatic control studies this fitting is good enough. We have data from 9 fermentation runs and we plan to use all of them to get an optimal fitting.

The model described above is highly nonlinear, open loop unstable, multivariable, with more manipulated variables than controlled variables and subjected to strong disturbances (heat generation). Therefore, the model captures many of the difficulties encountered in controlling real SSC bioreactors.

III. LINEAR PREDICTIVE CONTROL

This technique is useful to control multivariable plants with bounded inputs and subjected to unmeasured disturbances. The algorithm computes optimal control moves using a linear process model and taking into account the input constraints [Ogunnaike and Ray, 1994].

The control computation is performed in two stages: a) future controlled variables are estimated from past measurements and control moves, and b) an optimum trajectory is computed over a prediction horizon of P steps and applying C control moves (control horizon). At each sampling time, the whole procedure is repeated an only the first control move is applied to the plant, in a receding horizon form. P and C are tuning parameters. An additional useful feature of LMPC algorithms is that each input and output variable in the control structure can be weighted differently in the cost function, therefore, operational criteria can be directly incorporated into the control design.

The minimization problem in most LMPC algorithms can be formulated in the following form:

$$\min_{\Delta u_k,\ldots,\Delta u_{k+C-1}} \sum_{i=1}^{P} e_{k+i}\cdot W_D^e\cdot\left(e_{k+i}\right)^T + \sum_{i=1}^{C}\Delta u_{k+i-1}\cdot W_D^{\Delta u}\cdot\left(\Delta u_{k+i-1}\right)^T$$

s.t.

$$u_L \le u_{k+i-1} \le u_U\ ; \quad \forall\, i=1,\ldots,C$$

$$y_L \le \hat{y}_{k+i} \le y_U\ ; \quad \forall\, i=1,\ldots,P$$

$$\Delta u_{k+i} = 0\ ; \quad \forall\, i=C,\ldots,P$$

Here, $\hat{y}_k$ is the vector of predicted plant outputs at time interval k, e_k is the vector of output deviations from the set points and Δu_k is the vector of control moves. W_D^e and $W_D^{\Delta u}$ are diagonal matrices with weights that penalize the output deviations from the set points and the control movements respectively. Hence, by adequately tuning the weights, the process engineer can make some manipulated variables move more than others and get smaller deviations in some specified plant outputs. In addition, the prediction horizon, P, defines the period over which the cost function will be minimized; a large P assures a smooth and stable performance of the controller and should cover over 80% of the settling time. In turn, the control horizon, C, establishes the length of the sequence of future control moves; heuristics suggests that C << P. The minimization problem also includes constraints on inputs and outputs, therefore, in the expression above u_L and y_L represent the lower bounds, and u_U and y_U represent the upper bounds. This optimization problem do not have an analytical solution, save when a linear predictive model is used and no constraints are included, thus in the general case, the problem should be solved numerically.

There are few applications of LMPC to SSC processes reported in the literature. In [Paján et al., 1997], an unconstrained LMPC algorithm was assessed and compared with PID control in a simulated SSC bioreactor using a simple lumped parameter model. The predictive controller achieved much better performance, showing smaller overshoots, shorter settling times and a more robust behavior. However, the model used was theoretical without direct link with real data. Therefore, it was not possible to relate the simulation results with practical experience. Recently, [von Meien et al., 2004] applied LMPC and PID to control a simulated SSC bioreactor using a distributed parameter model. Here, LMPC allowed a significant improvement in the bioreactor productivity compared with PID control. Due to the explicit inclusion of heterogeneity and the deleterious effect of agitation, the model was able to reproduce a similar complex dynamics as observed in real SSC bioreactors.

[Fernández, 2001] applied unconstrained LMPC to control the SSC bioreactor described here. He obtained encouraging preliminary results, although it was not possible to achieve reproducible fermentation runs to validate the procedure. The experiments were expensive, fermentation runs lasted almost a week and the bioreactor was prone to contamination. In addition, the linear model obtained in a given run was not useful to control other runs, since each batch behaved differently. Therefore, preliminary simulation studies with a reliable model can be extremely useful to develop effective control strategies for SSC bioreactors.

IV. RESULTS

We report here simulation for the bed temperature control of the SSC bioreactor described above. Inlet air temperature, Tgi, relative humidity, Hgi, and flowrate, Ggi, were used as manipulated variables and constrained as in the real plant: Tgi (19-30ºC); Hgi (55-100%), and Ggi (50-200 kg/h).

The performance of the Linear Model Predictive Control (LMPC) was assessed using the MPC Matlab Toolbox and the MPC Graphical User Interface of [Ricker et al., 1998]. Since the LMPC algorithm uses a linearized model of the plant, here we consider a nominal constant trajectory defined by Tgi = 25ºC, Hgi = 85% and Ggi = 100 kg/h. The estimated equilibrium point was obtained with the TRIM function of Matlab, defining the time derivative of Tb as zero.

Open Loop Response

Fig. 8 compares the response of the nonlinear plant with the linearized plant in open loop operation, keeping the input variables constant in the values defined above. It can be seen that during the first 40 hours the responses of both models are extremely different; later the responses are very much alike. Therefore, the nonlinearity of the plant is more influential during the first half of the fermentation. In addition, it can be seen that without control the solid bed suffers an undesirable overheating.

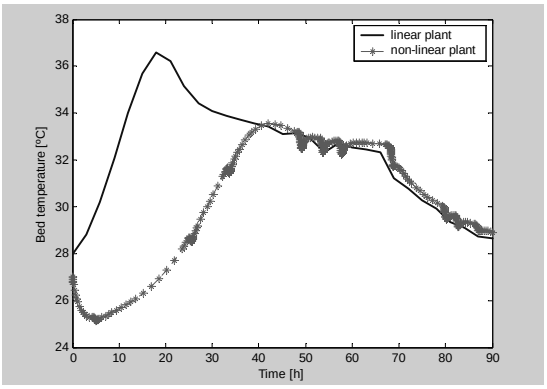

Fig. 8. Bed temperature (open loop simulation).

Closed Loop Response

The plant was first controlled with one manipulated variable at a time. In all these cases, the sample time was 5 min, the prediction horizon, P, was 12 sample times (60 min) and the control horizon, C, was 3 sample times (15 min). The input and output weights used in the simulations, are indicated in the captions of the respective figures.

Fig. 9 shows the results obtained by manipulating the inlet air temperature only. As seen in the figure, a good control cannot be attained here, since between hours 35 and 70 the input variable gets saturated (Fig. 9.a) and the bed temperature overpasses the set point (Fig. 9.b). We have observed this behavior in real SSC fermentations, although the low bound for the inlet temperature was lower. The model does not reproduce accurately the dynamic response of the real plant; hence we have to increase the lower bound in the simulations in order to achieve the same behavior. The observed peaks are associated with the fresh water added to control bed humidity. This water is added by pulses (not shown here).

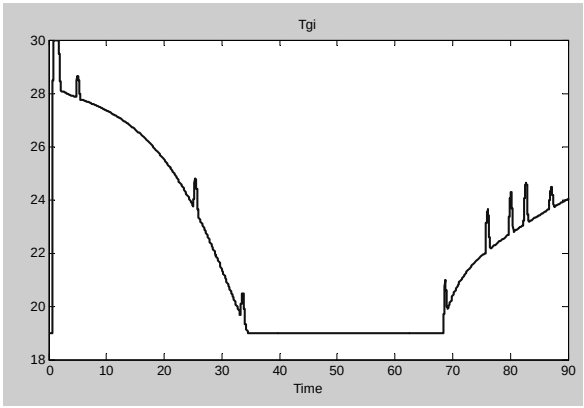

(a)

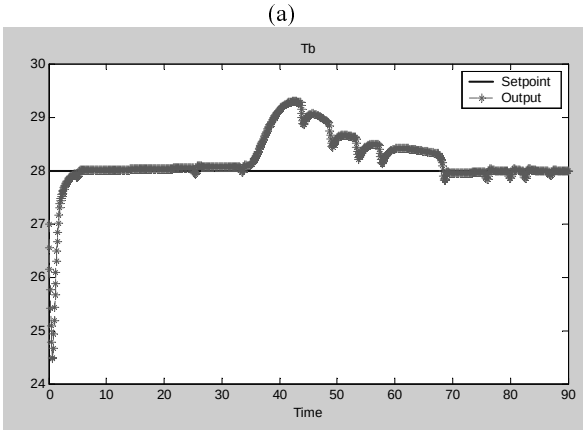

(b)

Fig. 9. Control using inlet air temperature only. (a) Manipulated variable with $w^{Tgi} = 0.1$; (b) Controlled variable with $w^{Tb} = 1$.

The results obtained by manipulating inlet air humidity only, are shown in Fig. 10. The control performance is worse in this case. The manipulated variable (Fig. 10.a)

remains saturated for longer periods and the bed temperature (Fig 10.b) reaches higher temperatures. In addition, during the initial stage, the bed takes longer to get to the reference temperature.

Controlling with inlet air flowrate is not good enough either. During most of the fermentation the input variable remains saturated (Fig. 11.a) and the bed temperature (Fig. 11.b) is almost never close to the set point.

Using two manipulated variables simultaneously is a much better approach. For example, Fig 12 shows the result obtained with the simultaneous manipulation of inlet air temperature and relative humidity.

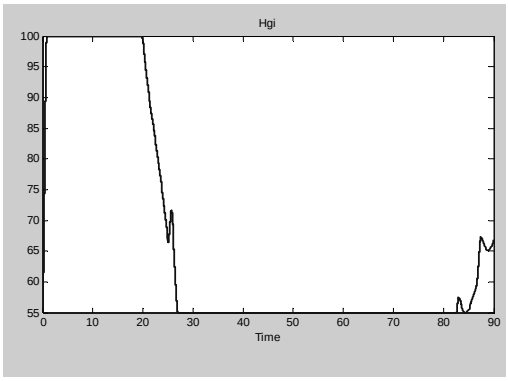

(a)

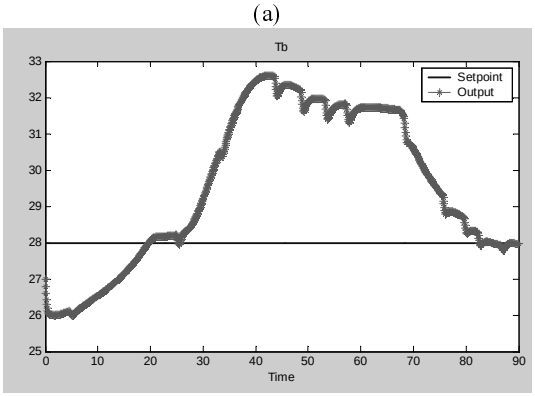

(b)

Fig. 10: Control using inlet air relative humidity. (a) Manipulated variable with $w^{Hgi} = 0.1$; (b) Controlled variable with $w^{Tb} = 1$.

Here, the bed temperature overshoot (Fig. 12.b) is less than 0.8ºC, although both manipulated variables (Fig. 12.a) remain saturated for more than 10 hours, as we have experienced in real SSC fermentations. This illustrates how difficult is to control the bed temperature.

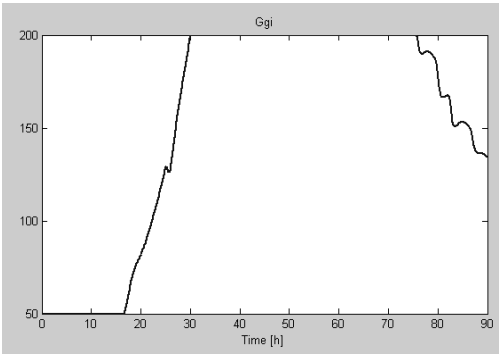

(a)

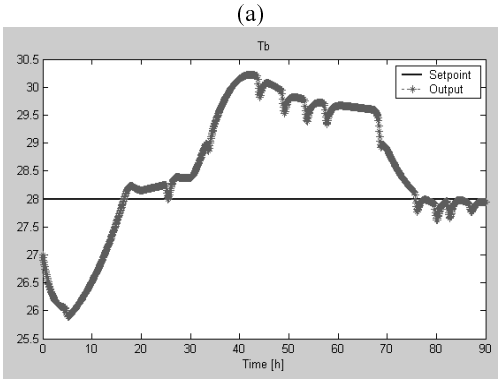

(b)

Fig. 11: Control using inlet air flow rate. (a) Manipulated variable with $w^{Ggi} = 0.1$; (b) Controlled variable with $w^{Tb} = 1$.

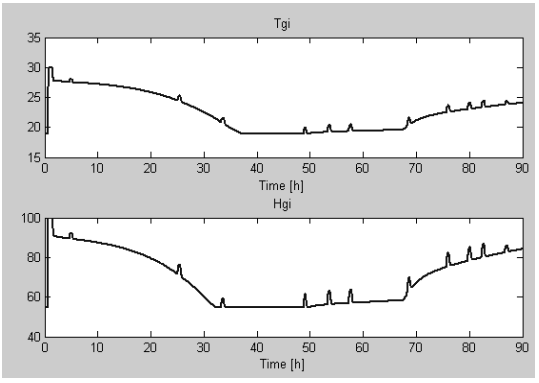

(a)

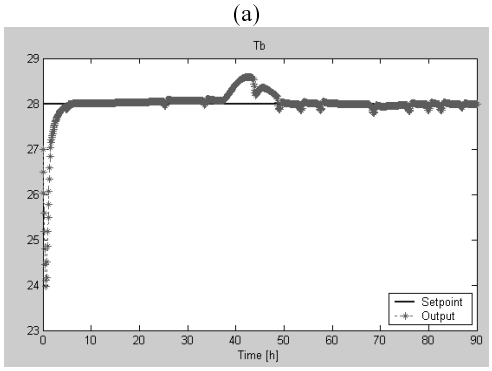

(b)

Fig. 12: Control using inlet air temperature and relative humidity. (a) Manipulated variables with $w^{Tgi} = 0.1$ and $w^{Hgi} = 0.01$; (b) Controlled variable with $w^{Tb} = 1$.

Figure 13 shows the control achieved with the simultaneous manipulation of inlet air temperature and flowrate. A better performance is observed here, with no input saturation (Fig. 13.a) and no temperature bed overshoot (Fig. 13.b). Real SSC fermentations in our pilot bioreactor did not show such a good control with inlet air flowrate manipulation. Hence, the sensitivity of the model to inlet air flowrate should be revised.

As expected, controlling with relative humidity and flowrate simultaneously presented larger bed temperature overshoots and longer saturation periods (not shown).

Finally, figure 14 shows the result obtained by manipulating the three input variables at the same time. This is by far the best case, with practically no saturation in temperature and humidity (Fig. 14.a) and a very good regulation (Fig. 14.b).

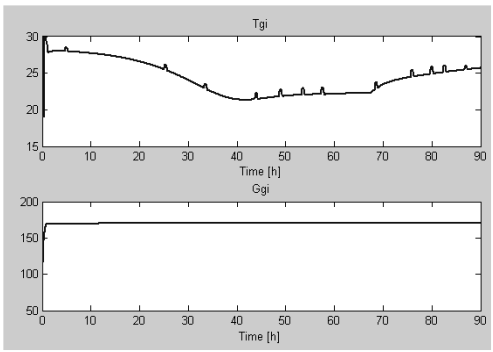

(a)

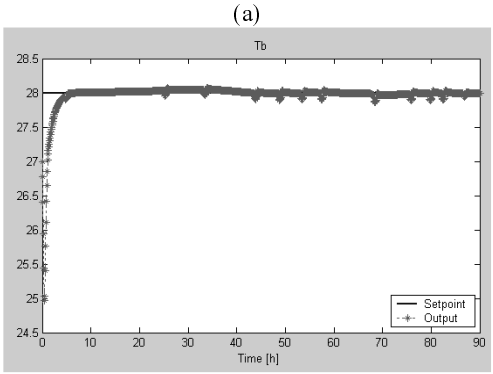

(b)

Fig. 13. Control using inlet air temperature and flow rate. (a) Manipulated variables with $w^{Tgi} = 0.1$ and $w^{Ggi} = 0.1$; (b) Controlled variable with $w^{Tb} = 1$.

V. CONCLUSIONS

It was verified that the developed model is able to qualitatively reproduce many of the control difficulties observed in real SSC fermentations. In addition, the control difficulties included in the model were overcome with LMPC. In particular, using two or three manipulated variables, a very good regulation can be achieved and input saturation is minimized.

The real plant presented other limitations not reproduced by the model, like heterogeneity (which produced strong temperature gradients) noisy measurements and strong unmeasured disturbances. Therefore, it is not clear if LMPC would be a good option under these conditions.

Future work includes optimal model fitting using least squares and data from 9 fermentation runs, developing and implementation of a noise model and application of several on line filtering procedures. The final aim is to develop a robust control system that could be applied with confidence in real SSC bioreactors.

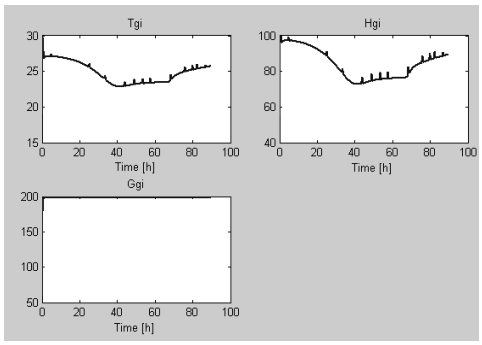

(a)

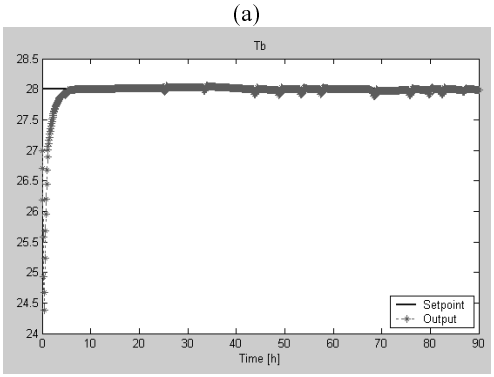

(b)

Fig. 14: Control using inlet air temperature, relative humidity and flow rate. (a) Manipulated variables with $w^{Tgi} = 0.1$, $w^{Hgi} = 0.01$ *and* $w^{Ggi} = 0.1$; (b) Controlled variable with $w^{Tb} = 1$.

ACKNOWLEDGEMENTS: This work was supported by project FONDECYT 1030325.

REFERENCES

[Fernández, 2001] M. A. Fernández, Control automático de un bioreactor piloto para cultivos sobre substrato sólido. PhD Thesis, Dpto. Ingeniería Eléctrica, Universidad de Chile, Santiago, 2001.

[Fernández et al., 1997] M. Fernández, J. Ananías, I. Solar, R. Pérez, L. Chiang and E. Agosin, "Advances in the development of a control system for a solid substrate pilot bioreactor," in Advances in Solid State Fermentation, B. K. L. S. Roussos, M. Raimboult, G. Viniegra-González, Eds. Dordrecht: Kluwer, 1997.

[Fainé, 2004] M. J. Fainé, Simulation and Internal Model Control of a pilot scale bioreactor for solid substrate cultivation, Dept. of Chemical and Bioprocess Engineering, P. Catholic University of Chile, 2004. (in Spanish)

[Gelmi, 2002] C. Gelmi, R. Pérez-Correa and E. Agosin, "Modelling *Gibberella fujikuroi* and GA_3 production in solid-state fermentation," *Proc. Biochem.* vol. 37, pp. 1033-1040, 2002.

[Lekanda and Pérez-Correa, 2004] S. Lekanda and J. R. Pérez-Correa, "Energy and water balances using kinetic modeling in a pilot-scale SSF bioreactor," *Proc. Biochem*. 2004 (in press)

[Nagel et al., 2000] F. Nagel, J. Tramper, M. Bakker, and A. Rinzema, "Model for on-line moisture-content control during solid-state fermentation". *Biotechnol. Bioeng.*, vol. 72, pp. 231-243, 2000.

[Ogunnaike and Ray, 19994] B. A-. Ogunnaike and W. H. Ray, Process Dynamics, Modeling, and Control, New York: Oxford University Press, 1994.

[Paján et al., 1997] H. Paján, R. Pérez-Correa, I. Solar and E. Agosin, "Multivariable model predictive control of a solid substrate pilot bioreactor: A simulation study," in Global Environmental Biotechnology, Donald L. Wise, Ed., Dordrecht: Kluwer, 1997, pp. 221-232.

[Peña y Lillo et al., 2001] M. Peña y Lillo, R. Pérez-Correa, E. Agosin and E. Latrille, "Indirect measurement of water content in an aseptic solid substrate cultivation pilot-scale bioreactor," *Biotechnol. Bioeng.*, vol. 76, pp. 44-51, 2001.

[Ricker et al., 1998] N. L. Ricker, M. Morari and A. Bemporad, "The MPC Graphical User Interface" Available in http://depts.washington.edu/control/LARRY/GUI/, 1998.

[Von Meien et al., 2004] O. F. von Meien, L. F. Luz Jr., D. A. Mitchell, R. Pérez-Correa, E. Agosin and J. Arcas, "Control strategies for intermittently-stirred, forcefuylly-aereated solid-state fermentation bioreactors on the analysis of a distributed parameter model", accepted for publication in *Chem. Eng. Science*, 2004.

APPENDIX

Table A1: Model parameter values

Parameter	Value	Units
A	11.78	[m^2]
$C_{p,a}$	1004.9215	[J/kg·K]
$C_{p,v}$	1867.3	[J/kg·K]
T_{wall}	28	[ºC]
$Y_{q/CO2}$	7023305.08	[J/h]
$Y_{X/CO2}$	0.55	[kgx/kgCO_2]
$Y_{x/Ni}$	30	[kgx/kgN]
$Y_{X/O2}$	0.9417	[kgx/kgO_2]
k	0.00192969	[1/h]
k_{exp}	1.1	[-]
k_g	0.38	[kgb.s/kgCO_2]
k_N	0.00129421	[1/kgN·kgb.s.]
k_w	1	[kgw/kgCO_2]
m_{CO2}	0.12120027	[kgCO_2/kgx·h]
m_{O2}	0.0554	[kgO_2/kgx·h]
λ_w	2432000	[J/kgw]
δ	0.0214	[1/h]
ϕ	0.04349194	[-]
σ	5.67E-08	[J/h·m^2·K^4]
μ_M	0.20694318	[1/h]
ξ	0.22	[-]